NANO LETTERS

2007
Vol. 7, No. 2
531−535

Effect of C_{60} on Solid Supported Lipid Bilayers

Tighe A. Spurlin and Andrew A. Gewirth*

Department of Chemistry at Urbana-Champaign, Urbana, Illinois 61802

Received September 27, 2006; Revised Manuscript Received December 19, 2006

ABSTRACT

We show that water-soluble fullerenes accumulate on the surface of zwitterionic and cationic supported bilayers to different extents. We propose on the basis of bilayer thicknesses, phase-transition temperatures, and fullerene movement that the water-soluble fullerenes do not penetrate into the hydrocarbon tails of supported bilayers. These findings are important to toxicity issues concerning fullerene materials and the development of decorated lipid bilayers for future drug delivery or sensor application.

The discovery of fullerenes in 1985,[1] the ability to produce larger quantities of fullerenes in the lab,[2,3] and their subsequent commercial availability have resulted in multiple applications for fullerene-based materials. Current proposed applications for fullerene-based nanomaterials involve items as varied as face creams,[4] drug delivery vehicles,[5,6] and mechanical lubricants.[7] The growing diversity of uses for nanomaterials has led to debate in both the scientific[8−11] and political[12,13] communities on their toxicological and environmental impact. The debate has arisen over whether current safety and disposal practices based on bulk material properties are applicable to nanomaterials of the same substance because nanosized materials can have different properties.[10,11]

The mechanism of their interaction with biological components must be ascertained in order to evaluate the toxicity of nanomaterials. In the particular case of fullerenes, several studies show that water-solubilzed fullerenes cause eukaryotic[9,14,15] and prokaryotic[16] cell death through the generation of reactive oxygen species.[10,15,17] However, other studies present evidence that water-solubilzed fullerenes actually protect lipids from oxidative damage and indicate that these materials are nontoxic.[8,18,19] In addition, little is known about the specific interaction of water-soluble fullerenes with lipid bilayers. In particular, the way in which water-soluble fullerenes interact with bilayers, including those with both charged and zwitterionic head groups, has never been evaluated. A fullerene−lipid association featuring fullerene intercalation into the bilayer leaflets or more dramatically featuring bilayer disruption clearly presents different consequences relative to one where the lipid−fullerene interaction is less strong. The location of water-soluble fullerene whether residing in the hydrophilic headgroup or the hydrophobic tails of lipid bilayers might be of importance to toxicity-related issues.[10,20] In this paper, we utilize in situ atomic force microscopy (AFM) to investigate the interaction of water-soluble C_{60} with supported lipid bilayers.

Supported lipid bilayers composed of pure zwitterionic 1,2-dimyristoyl-*sn*-glycero-3-phosphcholine (DMPC) and cationic 1,2-dimyristoyl-3-trimethylammonium-propane (DMTAP) were formed on freshly cleaved mica substrates and imaged before and after water-soluble fullerene exposure to ascertain fullerene−lipid interactions. To further elucidate fullerene−lipid interactions, fullerene-exposed DMPC bilayers were melted through the gel- to fluid-phase transition and examined with AFM and attenuated reflectance infrared spectroscopy (ATR-IR) to understand the effect fullerene adsorption had on lipid chain packing. Our findings show that water-soluble fullerenes adsorb to lipid headgroups and do not disrupt lipid hydrocarbon chain packing. Additionally, under identical conditions we observe a stronger interaction of water-soluble fullerenes with supported bilayers containing positively charged headgroups. These findings clarify the interactions between water-solubilized fullerenes and biological components, which relate to toxicity concerns. The findings also outline a method for decorating supported lipids with water-soluble fullerene aggregates for the potential development of delivery vehicles and sensors.

Lipid vesicles were prepared with ultrapure water (18.2 MΩ cm, Milli-Q UV plus, Millipore, Billerica, MA) adjusted to specific pHs with Na_2HPO_4 and $NaH_2PO_4{\cdot}H_2O$ at a concentration of 10 mM when necessary. Phosphate buffer salts (PBS) were obtained at purities of 99.9% or greater (Fisher Chemical). All lipids used in this study were purchased from Avanti Polar Lipids, Inc., and used without further purification. Supported lipid bilayers were formed utilizing the vesicle fusion technique pioneered by others[21] and described in detail by our group in previous publications.[22,23] C_{60} was obtained as a sublimed 99.9% pure powder

* Corresponding author. Tel: +1-217-333-8329; fax: +1-217-244-3186; e-mail: agewirth@uiuc.edu.

10.1021/nl0622707 CCC: $37.00
Published on Web 01/03/2007

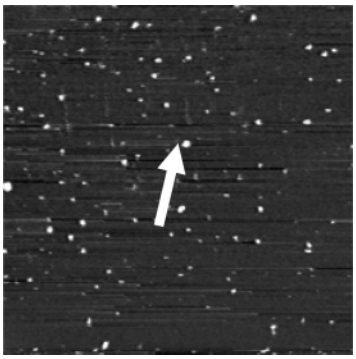

Figure 1. AFM of aqueous C_{60} on mica after exposure to 1 M NaCl. A white arrow points to a fullerene aggregate. The AFM image has x,y dimensions of 5×5 μm^2 and a z scale of 15 nm.

(MER Corporation). Water-soluble fullerenes (C_{60}) were prepared using freshly distilled tetrahydrofuran (THF) and ultrapure water using a literature procedure.[9,16,24] Briefly, fullerene powder was added to THF and stirred for 24 h to produce a dilute solution (9 mg C_{60}/mL THF)[9,24] of THF solubilized C_{60}. Milli-Q water was then added to the flask containing THF and C_{60}, which was heated to remove THF.[9,24] Complete extraction of C60 into the organic phase was verified by the absence of peaks observed in UV−visible spectra of the aqueous extract layer (see the Supporting Information).[24,25] UV−visible spectroscopy was also used to determine the concentration of C_{60} in this solution.[24,25]

Water-soluble fullerenes were further characterized with MALDI-TOF. The MALDI-TOF measurements revealed only a single peak at $m/z = 720$ (as shown in the Supporting Information) as expected for a single C_{60} molecule.[26,27] Atomic force microscopy (AFM) was used to analyze the height of fullerene aggregates. AFM images were collected using a MAC mode noncontact configuration described previously.[22] AFM images of 700 ppb C_{60} in pure water over mica showed no deposition. The addition of high concentrations of salt destabilizes the water-soluble fullerene aggregates and leads to their precipitation from solution.[16,24,28] Thus, we utilized the addition of 1 M NaCl to 700 ppb C_{60} solutions over mica substrates in an AFM solution cell to demonstrate aggregation of C_{60}. After incubation of 1 M NaCL and 700 ppb C_{60} in the solution cell for 12 h time, fullerene aggregates were observed on the mica surface as shown in Figure 1. The white arrow in Figure 1 points to a fullerene aggregate on the substrate. Aggregate heights ranged from 3 to 15 nm with a mean of 4.7 nm. According to the height we observe, a multilayer feature must be present on the mica surface because monolayers of pristine fullerene vapor deposited on substrates are reported to be ~1 nm tall.[29,30] The diameters of the aggregates ranged from 35 to 72 nm with a mean of 49.6 nm. However, the observed diameters of the fullerene aggregates are skewed to higher values as a result of convolution with the finite radius of the AFM tip (ca. 20−50 nm).[31,32]

Literature reports using various preparation and analysis methods of aqueous fullerene dispersions without salt report diameters ranging from 1 to 500 nm.[9,16,28,33,34] The addition of 0.001−0.05 M NaCl[16] had no effect on fullerene aggregate size over 15 weeks and no precipitation was observed. Addition of 0.7 M NaCl was observed to precipitate fullerene aggregates out after 48 h.[16] A related study[28] examining the stability of fullerene aggregates over a time period of 2 months reported that 1 M NaCl increased the mean hydrodynamic diameters of fullerene aggregates by more than a factor of 2.[9,16,28,33,34] The mean height of 4.7 nm for fullerene aggregates in the presence of 1 M NaCl observed here is consistent with these previous results.

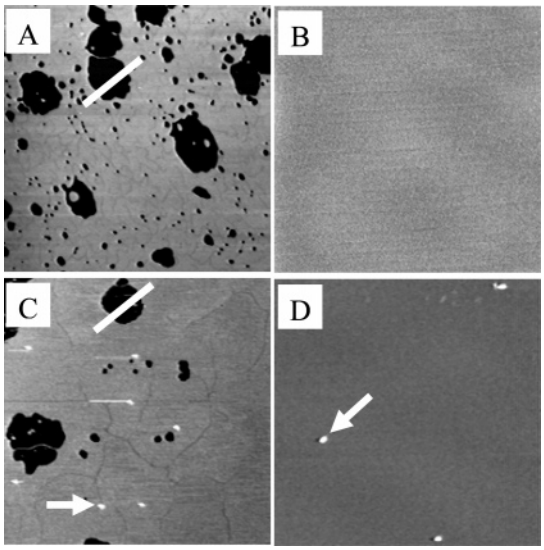

Figure 2. AFM of DMPC bilayer: (A) at 15 °C (gel phase) without C_{60}, (B) at 34 °C (liquid phase) without C_{60}, (C) at 15 °C (gel phase) with 2900 ppb C_{60}, and (D) at 32 °C (liquid phase) with 2900 ppb C_{60}. White lines bisect dark bilayer defects, and white arrows point to fullerene aggregates. All images are 5×5 μm^2 (x,y) at a z scale of 15 nm.

A DMPC bilayer prepared on a mica substrate in 10 mM pH 7.2 PBS buffer was imaged through the two phase-transition events reported previously.[22,35−37] Figure 2A and B shows the gel-phase DMPC bilayer and fluid-phase DMPC bilayer obtained at 15 and 34 °C, respectively. Thickness values of 4.4 ± 0.3 nm for the gel-phase DMPC bilayer were attained through cross-section analysis of defects in the bilayer surface, as illustrated by the white line bisecting a dark defect to the mica surface in Figure 2A. The first melting transition occurred over the range of 23−26 °C, and the second melting transition was observed over a range of 28−31 °C. As seen in Figure 2B, the DMPC bilayer formed a flat homogeneous bilayer after lipid expansion closed defects to the mica substrate during the melting transitions. The bilayer thickness,[22,38,39] phase-transition behavior,[22] and flat homogeneous liquid-phase bilayer morphology[37,40,41] appear as expected before water-soluble C_{60} addition, establishing that a well-formed bilayer has been created.

Figure 2C and D depicts images of the same bilayer in the gel and fluid phase, respectively, after incubation of 2900 ppb C_{60} in the solution cell for 2 h. The image shown in Figure 2C is similar to the image before exposure to C_{60} with 4.4 ± 0.3 nm deep bilayer defects. The phase-transition temperatures were unchanged, suggesting that water-soluble fullerenes, at least at the concentrations used in our study, do not effect lipid chain ordering. The main difference in

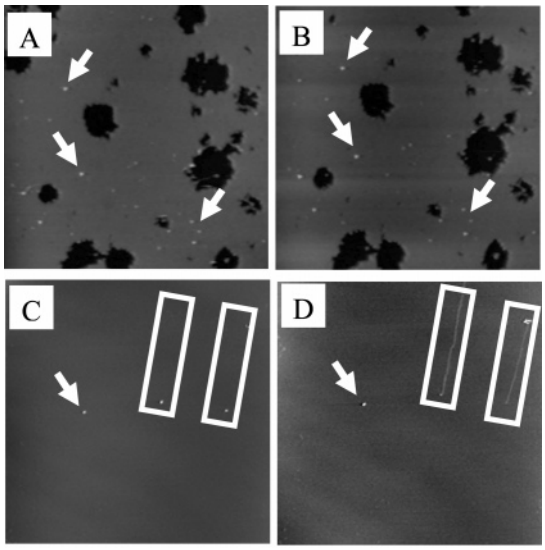

Figure 3. AFM images showing fullerene immobility on a gel-phase DMPC bilayer and mobility on a liquid-phase DMPC bilayer. Parts A and B were obtained for down and up scanning directions at 15 °C. Parts C and D were obtained for down and up scanning directions at 35 °C. White arrows point to immobile fullerene aggregates. White boxes depict movement path of fullerene aggregates. All images are 10 × 10 μm^2 (x,y) at a z scale of 15 nm.

images exposed to water-soluble fullerenes is the presence of white protrusions, highlighted by white arrows in Figure 2C and D, which extend 5.6 ± 1.1 nm above the bilayer plane. The tip-convolved diameters of these protrusions varied between 80 and 170 nm. The heights of the aggregates are within the range of heights (3−15 nm) observed for fullerene aggregates deposited on mica substrates under high salt conditions described above. In addition to aggregate height and diameter data, the gel-phase lipid area covered by fullerene aggregates was calculated from AFM images. Corrections were made to the calculations to account for lipid surface area discrepancies induced by differences in bilayer defect amounts. The fullerene aggregate coverage was observed to increase over time with 0.38 ± 0.26% of the lipid surface being covered with fullerene after 1 h and 1.49 ± 0.62% being covered after 11 h of 2900 ppb C_{60} incubation.

To further investigate the behavior of the fullerene aggregates on supported lipid bilayers, we captured images sequentially for DMPC bilayers in the gel phase, as they melted, and in the fluid phase after exposure to 2900 ppb C_{60}. Figure 3A and B illustrates the immobility of fullerene aggregates on gel-phase DMPC bilayers during AFM scanning in opposite directions. White arrows in Figure 3A and B points out several aggregates that do not move on the gel-phase bilayer during scanning. Alternatively, bilayer material inside the defects was observed to migrate, as discussed in a previous paper.[42] As DMPC bilayers melted at increased temperatures, fullerene aggregates became mobile (shown in the Supporting Information) either by diffusing with liquid-phase lipids or through interaction with the AFM tip. Figure 3C and D, obtained during AFM scans collected in opposite directions, demonstrates the movement of two fullerene aggregates on the liquid-phase DMPC bilayer. The white boxes show the movement of the aggregate in the two scans. A white arrow in Figure 3C and D points to an isolated aggregate that remained immobile on the bilayer surface.

The movement of fullerene aggregates on the liquid-phase supported lipid bilayer further suggests that the aggregates rest on top of lipid headgroups because no disruption of the underlying bilayer was observed. The exact movement mechanism of fullerenes on the supported bilayer is currently unknown; however, several references detail similar rolling and sliding movements for fullerene materials[43−45] and carbon nanotubes[46−49] under various conditions. In our experimental setup, it is likely that the AFM tip induces some of the movement observed because (1) aggregates were observed to accumulate outside the scanning window and (2) in certain instances aggregates were observed to roll in one direction, stop, and then roll back in the opposite direction depending on the tip scan direction.

On the basis of the insensitivity of the phase transition to fullerene addition and lack of damage to the bilayer with fullerene movement, we propose that water-soluble fullerene aggregates settle onto the supported bilayer and do not penetrate the hydrophilic headgroup region. In particular, the phase-transition invariance suggests that there is no change in lipid chain ordering upon fullerene addition. Support for this claim comes from ATR-IR spectroscopy (Supporting Information), which showed that the CH_2 (υ_s) band at 2850 cm^{-1} for gel-phase bilayers and 2853 cm^{-1} for liquid-phase bilayers were unchanged upon the addition of 2900 ppb water-soluble fullerene. This infrared band is a known measure of lipid acyl chain conformation and shifts to higher energy with increased chain disorder.[50,51] The insensitivity of the band to fullerene addition strongly supports the contention that the fullerene does not penetrate into the hydrocarbon tail of the bilayer.

Previous work examining the interaction of fullerenes with lipid bilayers found that fullerene aggregates in the lipid bilayer tail region[52,53] disrupt hydrocarbon chain packing of the lipids,[20,54] increase the electron permeability of lipid bilayers, and lead to a decrease in phase-transition temperature.[54] However, the fullerene−lipid constructs examined in this work do not indicate any disruption of lipid chain packing relative to the fullerene-free sample. Two possible explanations for the discrepancy between our findings and these previous reports are (1) the different preparative methods used in previous studies involving the co-hydration of dried fullerenes and lipid films[54−56] and (2) the use of fullerene powders in previous studies as opposed to water-dispersed fullerene aggregates used in our studies.

Electrophoretic mobility[16,25] and titration studies[25] show that water-dispersed fullerene aggregates carry a net negative charge, and two possible mechanisms for fullerene aggregate charge accumulation have been proposed.[16,25,57,58] We wondered whether this charge would enhance their interaction with a cationic lipid. Fullerene aggregates are known to interact with cationic fluorescent dyes[59] and cationic ions.[24,25,28]

Figure 4A and B shows AFM images of pure gel-phase DMTAP bilayers in Milli-Q water before and after the

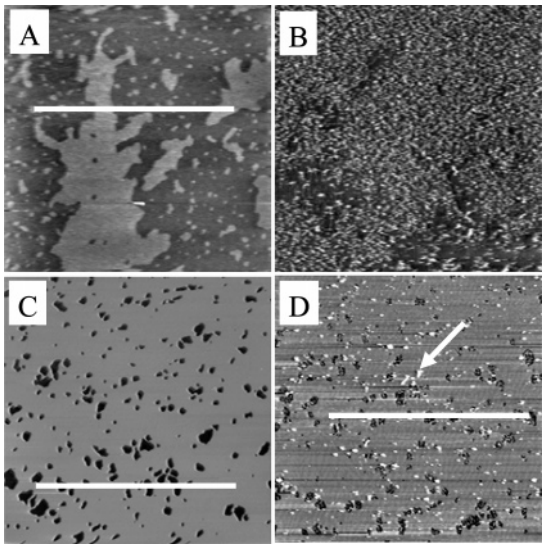

Figure 4. AFM comparison of DMTAP (A and B) and DMPC at 15 °C (C and D). Images A and C were taken before 700 ppb C_{60} addition, and images B, D were taken after incubation of 700 ppb C_{60} for 2 h. White lines in Figure 4A, C, and D depict cross-section analysis. A white arrow in Figure 4D points to a fullerene aggregate. All images are $10 \times 10\ \mu m^2$ (x,y) with a z scale of 15 nm. Bilayers were prepared in Milli-Q water with no additional salts.

addition of 700 ppb water-soluble C_{60} at 15 °C. Figure 4C and D provides images of gel-phase DMPC bilayers, before and after C_{60} addition, under the same conditions as images taken for DMTAP bilayer to allow a direct comparison of coverage amounts. Cross-section analysis, illustrated by a white line in Figure 4A, of DMTAP bilayers formed on mica substrates shows the expected presence of two solid phases with different chain tilt angles, which results in height differences of 1.1 ± 0.2 nm between the solid phases.[60−62] After confirmation of DMTAP bilayer formation, the bilayer was examined over time as 700 ppb C_{60} was incubated in the solution above the DMTAP bilayer. Over the course of 2 h, the DMTAP bilayer was observed to accumulate increased amounts of fullerene aggregates on the bilayer surface until no additional material was observed to accumulate. A representative image of DMTAP bilayers after incubation for 2 h with 700 ppb C_{60} is provided in Figure 4B. The fullerene material was determined to cover $45.4 \pm 3.7\%$ of the DMTAP bilayer surface after 2 h time.

Experiments undertaken with DMPC bilayers for comparison followed a similar method of confirming bilayer viability in Milli-Q water through cross-section analysis of images, as shown in Figure 4C, to record bilayer thicknesses of 4.6 ± 0.3 nm as expected. Well-formed DMPC bilayers were then exposed to 700 ppb water-soluble C_{60} for 2 h, while being imaged with the AFM. Figure 4D shows a DMPC bilayer after the incubation of 700 ppb C_{60} with a white arrow pointing to a fullerene aggregate on the bilayer. Fullerene aggregate coverage was observed to increase over time in a manner similar to DMTAP, albeit to a lesser extent with only $2.3 \pm 1\%$ of the lipid surface being covered. The adsorption of fullerenes to DMPC bilayers under Milli-Q water did not change the thickness, exactly as discussed earlier for DMPC bilayers in PBS.

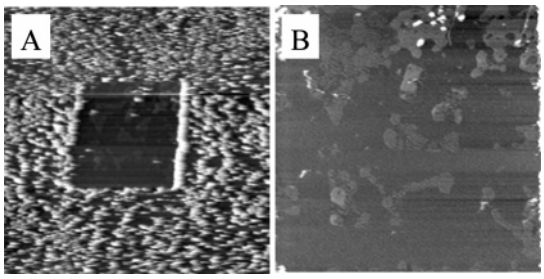

Figure 5. AFM scraping of C_{60} off of DMTAP. (A) MAC mode image of scraped square ($10 \times 10\ \mu m^2$). (B) MAC mode image of scrape area with C_{60} removed ($4 \times 4\ \mu m^2$). Both images shown with a z scale of 15 nm.

Coverage data obtained from Figure 4 show that fullerene aggregates settle onto cationic DMTAP bilayers to a greater extent than on the zwitterionic DMPC bilayers. This finding is to be expected because water-dispersed fullerenes are known to carry a net negative charge[16,25] and would be attracted to cationic lipid headgroups through electrostatic interactions. Fullerene aggregates are likely drawn to DMPC bilayers through a weaker interaction between the C_{60}^- and the dipole moment induced by the -N-$(CH_3)_3^+$ headgroup unit, such as that observed in previous molecular interactions with lipid headgroups.[63−65] The difference in attraction strength results in different coverage percentages observed over 2 h time.

Figure 5A and B shows that despite being heavily covered with fullerene aggregates DMTAP bilayers still exist intact under the fullerene layer. Figure 5A shows a $10 \times 10\ \mu m^2$ area of a DMTAP bilayer scraping away fullerene aggregates from a $4 \times 4\ \mu m^2$ area. Fullerene aggregate layer heights collected from AFM images by cross-section analysis were found to extend 6.3 ± 1.1 nm above the DMTAP bilayer plane. This height compares favorably with the height of fullerene aggregates, 5.6 ± 1.1 nm, on DMPC bilayers stated in a previous section. Figure 5B shows an image of the $4 \times 4\ \mu m^2$ area where C_{60} aggregates have been removed. Cross-section analysis of the bilayer underneath fullerene aggregates indicates that the DMTAP bilayer has a morphology with gel-phase domains differing in height by 1.2 ± 0.2 nm as observed for DMTAP bilayers without C_{60} (Figure 4A). This data along with similar results discussed above for DMPC bilayers show that most of the water-soluble C_{60} adhere to the headgroup portion of the lipid molecules without drastically altering the underlying bilayer.

To summarize, we have shown that water-dispersed fullerenes adhere to supported lipid bilayers containing zwitterionic lipid headgroups or cationic lipid headgroups. Negatively charged fullerene aggregates were observed to accumulate onto supported lipid bilayers consisting of cationic lipid headgroups to a greater extent than bilayers consisting of only zwitterionic lipid headgroups under the same conditions. We propose that fullerene aggregates interact only with the lipid headgroups and do not penetrate into the lipid hydrocarbon chains based on data indicating no alteration of bilayer thicknesses, phase-transition temperatures, and underlying bilayer morphology during fullerene movement and detachment. These findings are relevant to

the basic interactions water-dispersed fullerenes have with both zwitterionic lipids in membranes and charged molecules, such as proteins, near membrane surfaces.

Acknowledgment. We thank Professor Steven C. Zimmerman's group at the University of Illinois Urbana-Champaign for the use of distillation equipment for tetrahydrofuran preparation. We are grateful to the School of Chemical Sciences for use of the Mass Spectrometry Laboratory. The Voyager-DE STR mass spectrometer was purchased in part with a grant from the Division of Research Resources, National Institutes of Health (RR 11966). This work was supported by the NSF (CHE06-01952).

Supporting Information Available: Additional UV−vis, MALDI-TOF, ATR-IR, and AFM data figures. This material is available free of charge via the Internet at http://pubs.acs.org.

References

(1) Kroto, H. W.; Heath, J. R.; O'Brien, S. C.; Curl, R. F.; Smalley, R. E. *Nature* **1985**, *318*, 162.
(2) Kraetschmer, W.; Fostiropoulos, K.; Huffman, D. R. *Chem. Phys. Lett.* **1990**, *170*, 167.
(3) Kraetschmer, W.; Lamb, L. D.; Fostiropoulos, K.; Huffman, D. R. *Nature* **1990**, *347*, 354.
(4) Halford, B. *Chem. Eng. News* **2006**, *84*, 47.
(5) Ashcroft, J. M.; Tsyboulski, D. A.; Hartman, K. B.; Zakharian, T. Y.; Marks, J. W.; Weisman, R. B.; Rosenblum, M. G.; Wilson, L. J. *Chem. Commun.* **2006**, 3004.
(6) Zakharian, T. Y.; Seryshev, A.; Sitharaman, B.; Gilbert, B. E.; Knight, V.; Wilson, L. J. *J. Am. Chem. Soc.* **2005**, *127*, 12508.
(7) Luethi, R.; Meyer, E.; Haefke, H.; Howald, L.; Gutmannsbauer, W.; Guentherodt, H. J. *Science* **1994**, *266*, 1979.
(8) Gharbi, N.; Pressac, M.; Hadchouel, M.; Szwarc, H.; Wilson, S. R.; Moussa, F. *Nano Lett.* **2005**, *5*, 2578.
(9) Sayes, C. M.; Fortner, J. D.; Guo, W.; Lyon, D.; Boyd, A. M.; Ausman, K. D.; Tao, Y. J.; Sitharaman, B.; Wilson, L. J.; Hughes, J. B.; West, J. L.; Colvin, V. L. *Nano Lett.* **2004**, *4*, 1881.
(10) Nel, A.; Xia, T.; Maedler, L.; Li, N. *Science* **2006**, *311*, 622.
(11) Colvin, V. L. *Nat. Biotechnol.* **2003**, *21*, 1166.
(12) Thayer, A. *Chem. Eng. News* **2006**, *84*, 10.
(13) Morrissey, S. *Chem. Eng. News* **2005**, *83*, 46.
(14) Tsuchiya, T.; Oguri, I.; Yamakoshi, Y. N.; Miyata, N. *FEBS Lett.* **1996**, *393*, 139.
(15) Sayes, C. M.; Gobin, A. M.; Ausman, K. D.; Mendez, J.; West, J. L.; Colvin, V. L. *Biomaterials* **2005**, *26*, 7587.
(16) Fortner, J. D.; Lyon, D. Y.; Sayes, C. M.; Boyd, A. M.; Falkner, J. C.; Hotze, E. M.; Alemany, L. B.; Tao, Y. J.; Guo, W.; Ausman, K. D.; Colvin, V. L.; Hughes, J. B. *Environ. Sci. Technol.* **2005**, *39*, 4307.
(17) Kamat, J. P.; Devasagayam, T. P. A.; Priyadarsini, K. I.; Mohan, H. *Toxicology* **2000**, *155*, 55.
(18) Andrievsky, G.; Klochkov, V.; Derevyanchenko, L. *Fullerenes, Nanotubes, Carbon Nanostruct.* **2005**, *13*, 363.
(19) Sirotkin, A. K.; Zarubaev, V. V.; Poznyiakova, L. N.; Dumpis, M. A.; Muravieva, T. D.; Krisko, T. K.; Belousova, I. M.; Kiselev, O. I.; Piotrovsky, L. B. *Fullerenes, Nanotubes, Carbon Nanostruct.* **2006**, *14*, 327.
(20) Chang, R.; Violi, A. *J. Phys. Chem. B* **2006**, *110*, 5073.
(21) Tamm, L. K.; McConnell, H. M. *Biophys. J.* **1985**, *47*, 105.
(22) Feng, Z. V.; Spurlin, T. A.; Gewirth, A. A. *Biophys. J.* **2005**, *88*, 2154.
(23) Xie, A. F.; Yamada, R.; Gewirth, A. A.; Granick, S. *Phys. Rev. Lett.* **2002**, *89*, 246103/1.
(24) Deguchi, S.; Alargova, R. G.; Tsujii, K. *Langmuir* **2001**, *17*, 6013.
(25) Andrievsky, G. V.; Klochkov, V. K.; Bordyuh, A. B.; Dovbeshko, G. I. *Chem. Phys. Lett.* **2002**, *364*, 8.
(26) Ko, W.-B.; Heo, J.-Y.; Nam, J.-H.; Lee, K.-B. *Ultrasonics* **2004**, *41*, 727.
(27) Andrievsky, G. V.; Kosevich, M. V.; Vovk, O. M.; Shelkovsky, V. S.; Vashchenko, L. A. *J. Chem. Soc., Chem. Commun.* **1995**, 1281.
(28) Brant, J.; Lecoanet, H.; Wiesner, M. R. *J. Nanopart. Res.* **2005**, *7*, 545.
(29) Okita, S.; Miura, K. *Nano Lett.* **2001**, *1*, 101.
(30) Yase, K.; Ara-Kato, N.; Hanada, T.; Takiguchi, H.; Yoshida, Y.; Back, G.; Abe, K.; Tanigaki, N. *Thin Solid Films* **1998**, *331*, 131.
(31) Villarrubia, J. S. *Surf. Sci.* **1994**, *321*, 287.
(32) Markiewicz, P.; Goh, M. C. *Langmuir* **1994**, *10*, 5.
(33) Saha, A.; Mukherjee Asok, K. *J. Chem. Phys.* **2005**, *122*, 184504.
(34) Avdeev, M. V.; Khokhryakov, A. A.; Tropin, T. V.; Andrievsky, G. V.; Klochkov, V. K.; Derevyanchenko, L. I.; Rosta, L.; Garamus, V. M.; Priezzhev, V. B.; Korobov, M. V.; Aksenov, V. L. *Langmuir* **2004**, *20*, 4363.
(35) Keller, D.; Larsen, N. B.; Moeller, I. M.; Mouritsen, O. G. *Phys. Rev. Lett.* **2005**, *94*, 025701/1.
(36) Yang, J.; Appleyard, J. *J. Phys. Chem. B* **2000**, *104*, 8097.
(37) Leonenko, Z. V.; Finot, E.; Ma, H.; Dahms, T. E. S.; Cramb, D. T. *Biophys. J.* **2004**, *86*, 3783.
(38) Tristram-Nagle, S.; Liu, Y.; Legleiter, J.; Nagle, J. F. *Biophys. J.* **2002**, *83*, 3324.
(39) Johnson, S. J.; Bayerl, T. M.; McDermott, D. C.; Adam, G. W.; Rennie, A. R.; Thomas, R. K.; Sackmann, E. *Biophys. J.* **1991**, *59*, 289.
(40) Milhiet, P.-E.; Giocondi, M.-C.; Baghdadi, O.; Ronzon, F.; Le Grimellec, C.; Roux, B. *Single Mol.* **2002**, *3*, 135.
(41) Reviakine, I.; Simon, A.; Brisson, A. *Langmuir* **2000**, *16*, 1473.
(42) Feng, Z. V.; Granick, S.; Gewirth, A. A. *Langmuir* **2004**, *20*, 8796.
(43) Shirai, Y.; Osgood, A. J.; Zhao, Y.; Yao, Y.; Saudan, L.; Yang, H.; Chiu, Y.-H.; Alemany, L. B.; Sasaki, T.; Morin, J.-F.; Guerrero, J. M.; Kelly, K. F.; Tour, J. M. *J. Am. Chem. Soc.* **2006**, *128*, 4854.
(44) Shirai, Y.; Osgood, A. J.; Zhao, Y.; Kelly, K. F.; Tour, J. M. *Nano Lett.* **2005**, *5*, 2330.
(45) Hobbs, C.; Kantorovich, L. *Nanotechnology* **2004**, *15*, S1.
(46) Falvo, M. R.; Taylor, R. M., II; Helser, A.; Chi, V.; Brooks, F. P., Jr.; Washburn, S.; Superfine, R. *Nature* **1999**, *397*, 236.
(47) Miura, K.; Takagi, T.; Kamiya, S.; Sahashi, T.; Yamauchi, M. *Nano Lett.* **2001**, *1*, 161.
(48) Keeling, D. L.; Humphry, M. J.; Fawcett, R. H. J.; Beton, P. H.; Hobbs, C.; Kantorovich, L. *Phys. Rev. Lett.* **2005**, *94*, 146104/1.
(49) Buldum, A.; Lu, J. P. *Phys. Rev. Lett.* **1999**, *83*, 5050.
(50) Mantsch, H. H.; McElhaney, R. N. *Chem. Phys. Lipids* **1991**, *57*, 213.
(51) Le Bihan, T.; Pezolet, M. *Chem. Phys. Lipids* **1998**, *94*, 13.
(52) Nagle, J. F.; Tristram-Nagle, S. *Biochim. Biophys. Acta* **2000**, *1469*, 159.
(53) Tristram-Nagle, S.; Nagle, J. F. *Chem. Phys. Lipids* **2004**, *127*, 3.
(54) Jeng, U. S.; Hsu, C.-H.; Lin, T.-L.; Wu, C.-M.; Chen, H.-L.; Tai, L.-A.; Hwang, K.-C. *Physica B* **2005**, *357*, 193.
(55) Beeby, A.; Eastoe, J.; Heenan, R. K. *J. Chem. Soc., Chem. Commun.* **1994**, 173.
(56) Li, H.; Jia, X.; Li, Y.; Shi, X.; Hao, J. *J. Phys. Chem. B* **2006**, *110*, 68.
(57) Yamachika, R.; Grobis, M.; Wachowiak, A.; Crommie, M. F. *Science* **2004**, *304*, 281.
(58) Li, J.; Takeuchi, A.; Ozawa, M.; Li, X.; Saigo, K.; Kitazawa, K. *J. Chem. Soc., Chem. Commun.* **1993**, 1784.
(59) McHedlov-Petrossyan, N. O.; Klochkov, V. K.; Andrievsky, G. V.; Ishchenko, A. A. *Chem. Phys. Lett.* **2001**, *341*, 237.
(60) McKiernan, A. E.; Ratto, T. V.; Longo, M. L. *Biophys. J.* **2000**, *79*, 2605.
(61) Leonenko, Z. V.; Merkle, D.; Lees-Miller, S. P.; Cramb, D. T. *Langmuir* **2002**, *18*, 4873.
(62) Leonenko, Z.; Cramb, D. *Nano Lett.* **2002**, *2*, 305.
(63) Xie, A. F.; Granick, S. *Nat. Mater.* **2002**, *1*, 129.
(64) Mecke, A.; Uppuluri, S.; Sassanella, T. M.; Lee, D.-K.; Ramamoorthy, A.; Baker, J. R.; Orr, B. G.; Banaszak Holl, M. M. *Chem. Phys. Lipids* **2004**, *132*, 3.
(65) Scherer, P. G.; Seelig, J. *Biochemistry* **1989**, *28*, 7720.

NL0622707